Journal of
Materials Chemistry B

Materials for biology and medicine

Accepted Manuscript

This article can be cited before page numbers have been issued, to do this please use: Z. Yin, H. Cui, Q. Shu, C. Jin, Y. lin, J. Su, H. Huang, S. F. Liao, G. Ma, N. Hong, Y. Jiang and H. Fan, *J. Mater. Chem. B*, 2020, DOI: 10.1039/D0TB00204F.

ROYAL SOCIETY OF CHEMISTRY

rsc.li/materials-b

View Article Online
DOI: 10.1039/D0TB00204F

Multi-signal amplification electrochemical DNA biosensor based on exonuclease III and tetraferrocene

Zhaojiang Yin [#a] , Hanfeng Cui [#a] , Qingxia Shu [a], Chen Jin [a] , Yan Lin [a] , Jia Su [b] , HuiLian Huang [a] , Fusheng Liao [a] , Guangqiang Ma [a] , Nian Hong [a] , Yunfeng Jiang *[a], Hao Fan *[a]

[#] Contributed to this work equally

* Corresponding Author

The Affiliated Hospital, Department of Pharmacy, JiangXi University of Traditional Chinese Medicine, JiangXi 330004, China[a]

South University of Science and Technology of China, Shenzhen 518055, China[b]

E-mail addresses: 254240787@qq.com (Yunfeng Jiang), fanhao11@aliyun.com (Hao Fan)

Highlights

- A new and efficient signal marker, 3,5-bis(3, 5-bisferrocenethoxybenzyloxy) benzoic acid, firstly synthesized and used for labeling
- Based on the distinction between graphene and single-double stranded DNA, a homogeneous electrochemical sensor was constructed
- Exo III-assisted for cycling digestion, and the tetraferrocene -labeled probe chain is adsorbed onto the electrode to increase the signal

Abstract

Homogeneous electrochemical DNA biosensor's unique qualities have been of great interest to researchers, mainly due to its high recognition efficiency in solutions. However, the process of introducing additional markers and extra operations to obtain a signal are tedious and time consuming, which limits their overall potential applications. Herein, a novel tetraferrocene was synthesized and used as homogeneous electrochemical DNA biosensor probe label. It contains four ferrocene units that provide a greater signaling potential compared to monoferrocene, Furthermore, the target DNA triggers the cycle of double hairpin DNA probe with the aid of exonuclease III, promoting short single stranded DNA probe formation. The combination of the incorporated tetraferrocene labeled short DNA probe strands and graphene's ability to adsorption single stranded DNA, the hybridization process can transform in an electrode signal provided by tetraferrocene. A low detection limit of 8.2 fM toward target DNA with excellent selectivity was achieved. The proposed sensing system avoids tedious and time-consuming steps of DNA

modification, making the experimental processes simpler and convenient. The advantages of high sensitivity, selectivity and simple operation, makes this strategy applicable to DNA detection.

Keywords: Multiple signal amplification, Homogeneous, DNA detection, Tetraferrocene, Exonuclease III

1. Introduction

Gene sequence is the fundamental study of life sciences, and qualitative testing of specific genes is crucial for clinical, environmental, and food safety [1, 2]. For the past few decades, nucleic acids detection has relied on sensitive and effective DNA probing methods [3, 4, 5]. Methods of DNA detection can be converted into a quantified signal using transducers, such as optical, electrochemical, piezoelectric and thermal detection. Among these techniques, electrochemical sensors are regarded as an ideal approach due to their high sensitivity, inherent simplicity and miniaturization while avoiding disadvantages such as extravagant detection costs [6].

Currently, the preparation of electrochemical sensors involves DNA probe immobilization, which can lead to numerous drawbacks. These include laborious and time consuming processes, as well as a decrease in recognition efficiency that influences identification of steric hindrance and electron transfer [7, 8]. Furthermore, in order to obtain higher sensitivity, electrochemical sensors may require additional reagents and complex operations [9], which fail to achieve fast detection and entails higher costs. In order to combat these issues we attempted to develop a homogeneous electrochemical strategy by utilizing tetraferrocene as an electronic expansion unit, allowing the enhancement of sensitivity and rapid detection of DNA.

Graphene has been of great interest in the field of material science [10, 11, 12] owing to its high specific surface area [13], electrical conductivity [14], excellent pliability [15, 16], making it a promising material for applications in conductivity. Additionally, single and double stranded DNA could be effectively distinguishable on the surface of graphene through π–π stacking interaction between the conjugated π bonds of the nucleotide bases [17, 18]. This type of distinction usually involves fluorescence DNA detection [19, 20, 21], with homogeneous electrochemical DNA sensors rarely been investigated. Herein, graphene is employed as a functional electrode in a homogeneous electrochemical biosensor. The developed sensors not only distinguish between DNA chains, but

View Article Online
DOI: 10.1039/D0TB00204F

also use the characteristic electrical conductivity effective in order to enhance the redox properties of the redox marker.

Ferrocene is a redox active substance, and commonly used as an electrochemical DNA marker. Other DNA makers such as nanoparticles [22], enzyme [23] and metal-organic frameworks (MOFs) [24] require additional substrates or manipulation to obtain target signal. Ferrocene receives the analyst's barley that can get the signal directly in the physiological buffer solution requiring no addition reagents or target labeling [25, 26, 27, 28]. Nevertheless, each redox process of ferrocene involves a gain or loss of a single electron, with the electronic signals limiting the sensitivity of detection. In order to enhance efficiency, the strategy of probe modification via two ferrocenes units has been reported for DNA detection [29, 30]. Considering ferrocene's excellent properties we first synthesized tetraferrocene as a DNA probe marker. To the best of our knowledge, our prepared marker has the largest number of ferrocene units, capable of providing double the electrical signals.

This study shows an efficient homogeneous graphene-based electrochemical biosensor with tetraferrocene label DNA probe and exonuclease III (Exo III) -assisted cleavage amplification for the detection of target DNA. Scheme 1 displays a dual-stem loop structure probe (P1) that was the 5'-modified tetraferrocene has been prepared and the probe contained sequences which are partially complementary to target DNA. Initially, the probe resisted attachment to the graphene electrode surface due to the lack of base exposure in solution resulting in weak π–π stacking force. However, in the presence of the target DNA (T1), the loop-stem structure of the probe independently cross-opens via hybridization with target DNA generating double stranded DNA. Moreover, enzyme addition system is an effective catalytic tool for the amplification of the detection signal of target DNA, where enzymatic cleavage reaction of Exo III promotes stepwise removal of a single nucleotide from the blunt 3'-end of DNA duplexes releasing the target DNA (T1) and straight chain probe DNA (P1). Finally, target DNA is repeated in cooperation with enzymes, the massive recycling single chain element with tetraferrocene-labeled probe terminal was adsorbed and transferred to the electrode. Therefore, one type of ultrasensitive homogeneous electrochemical system, which indicates a rapid and low-cost homogeneous electrochemical sensor for target event detect was successfully prepared.

View Article Online
DOI: 10.1039/D0TB00204F

Scheme 1

2. Experiment

2.1. Chemicals and materials: Graphene (99.999%) was purchased from Nanjing Xianfeng Nano Material Technology Co., Ltd (Nanjing, China). ExoⅢ was purchased from Shanghai Sangon Biological Engineering Technology and Services Co., Ltd (Shanghai, China). The probe DNA labeled with Tatreferrocene (TtFc) at 5'-terminal and target DNA were synthesized, HPLC purified, and freeze-dried by Shanghai Sangon Biological Engineering Technology and Services Co., Ltd (Shanghai, China). The probe sequence and target sequence were respectively listed as follows;

Probe DNA (P1)：3'-ATTTCCGCAAGCGGCTGACGTCTTATATTGACG-Tetraferrocene-5'

Target DNA (T1)：3'-TTTACGTCAGCCGCTTGCGGAAAT-5'

single-base-mismatch DNA：3'-TTTACGTCAACCGCTTGCGGAAAT-5'

three-base-mismatch DNA：3'-TTTACGTTTTCCGCTTGCGGAAAT-5'

non-complementary DNA：3'-CCCGTACAGAAATAGGAATTCCCG -5'

HCl, NaCl, KCl, $MgCl_2$ and other reagents of analytical grade were purchased from Dingguo Biotechnology Inc. (Shanghai, China). All were used without further purification or treatment. Ultrapure water (18.2 MΩ.cm) was obtained from a Milli-Q water purification system and for all experiments.

2.2. Apparatus: Transmission electron microscopy (TEM) images were collected using FEI Tecnat tm Spirit TEM (America). TEM opened at an accelerating voltage of 80 kV. Scanning electron microscopy (SEM) images were obtained using a FEI Quanta250 field emission SEM system (America). All electrochemical experiments were performed in autolab electrochemical workstation (Metrohm Instruments Co., Swiss) using a standard three-electrode system, where the bare or modified GCE electrode (CHI104, Φ = 3 mm, CH Instruments, Inc. Shanghai) acted as the working electrode, Ag/AgCl electrode as the reference electrode and platinum wire as the counter electrode, respectively. All prepared DNA concentrations were determined by nanodrop 2000 spectrophotometer (Thermo Fisher Scientific, US).

2.3. Synthesis of tetraferrocene: α-Chloroacetylferrocene (**2**) was prepared by standard Friedel-Crafts-type acylation of ferrocene with chloroacetyl chloride [31], and then reduced to 2-chloroethylferrocene (**3**) by lithium aluminium tetrahydride and anhydrous aluminum chloride [32]. Methyl 3,5-bisferrocenethoxybenzoate (**5**) was obtained via nucleophilic substitution with methyl 3,5-dihydroxybenzoate (**4**) using potassium carbonate and potassium iodide as catalysts [33]. This was then reduced to (3,5-bisferrocenethoxyphenyl) methanol (**6**) using lithium aluminium tetrahydride in anhydrous diethyl ether [34], which was treated with triphenylphosphine and carbon tetrachloride to give 3,5-bisferrocenethoxybenzyl chloride (**7**) [35]. Subsequent nucleophilic substitution with methyl 3, 5-dihydroxybenzoate under standard conditions generated methyl 3,5-bis(3,5-bisferrocenethoxybenzyloxy)benzoate (**8**) in good yield [36]. Finally, cleavage of the ester moiety was conducted using sodium hydroxide in a mixture of methanol and tetrahydrofuran, giving 3,5-bis (3,5-bisferrocenethoxybenzyloxy) benzoic acid (**9**) (tetraferrocene) [37] (please see support information (SI) for further details).

Scheme 2

2.4. Preparation of graphene and modified electrode: Nanographene was prepared using the ball-milling method [38]. Steel balls (60 g) and graphite powder (2.0 g, diameter 1–1.3 cm) were placed into a hardened steel vial and purged with high-purity argon (99.999%) for 20 min before the vials were sealed and milled at 450 rpm for 20 h. The prepared graphene was described by TEM and SEM.

Figure 1

TEM image of graphene sheets (Figure 1A) shows flake-like shapes of graphene with ripples and edges. SEM images (Figure 1B) characterize the morphology and microscopic material of graphene's surface on glassy carbon, respectively. The graphene film exhibits uniform morphology over large areas with unique wrinkles on the surface, which greatly increases GCE surface area. Prior to the operation steps, GCEs were polished by aqueous alumina slurries with 0.3 μm particle sizes and 0.05 μm microcloth, followed by rinsing thoroughly with ultrapure water and ethanol. Graphene (0.5 mg) was dispersed in DMF (500 μL) solution and ultrasonicated for 1 h. Graphene–DMF dispersions (10 mL) were dropped onto GCE and allowed to dry at room

View Article Online
DOI: 10.1039/D0TB00204F

temperature for 6 h to obtain the graphene modified GCE.

2.5. DNA detection and electrochemical measurements: After optimization of the test conditions, the analytical procedure of the homogeneous electrochemical biosensor is as follows: Firstly, probe DNA was placed in 10 mM phosphate buffer saline at 95 °C for 10 min, followed by cooling to room temperature at a rate of 1 °C min^{-1}. Secondly, ExoⅢ-assisted target-analog recycling was performed in a homogeneous solution (300 μL) consisting of 0.7 μM P1, 20U ExoⅢ in buffer (50 mM KAc, 10 mM $Mg(Ac)_2$, 20 mM Tris-Ac, 1 mM dithiothreitol, pH 7.9). Adding target DNA to solution and the mixture allowed to reaction for the specified time at 37 °C in a constant temperature incubator. The mixture (100 μL) was placed onto graphene/GCE and incubated at room temperature for 15 min, followed by thorough rinsing with ultrapure water. Furthermore, a large number of TtFc-ssDNA adsorbed on graphene was detected by differential pulse voltammetry. The sample average of three tests was calculated for the final analysis of the results. Differential pulse voltammetry (DPV) was carried out in 0.1 M pH 7.4 phosphate buffered saline (PBS) solution and immediately performed from 0.0 to 0.7 V (Incr E0.004 V, amplitude 0.025 V, pulse width 0.05 s, pulse period 0.5 s), resulting in an electrochemical signal due to redox of tetraferrocene.

2.6. Electrophoresis demonstration of the amplification strategy: Polyacrylamide gel electrophoresis was analyzed to confirm and characterize the formation of the hybrid product in the designed electrochemical DNA sensor. In PAGE assay, four samples were prepared: 4 μM P1, 4 μM T1, a mixture of P1 incubated with T1 for 2 h at 37 °C without and with 10 μM ExoⅢ, respectively. The samples were loaded onto 16% nondenaturing polyacrylamide gel and run at room temperature in 1×TBE buffer (9 mM Tris-HCl, pH 7.9, 9 mM boric acid, 0.2 mM EDTA) at 120 V for 100 min. Then, the gel was stained with Gelred for 30 min and visualized under UV light, and photographed using the gel imaging system.

3. Results and discussion

3.1. The characterize of gaphene on the electrode: Electrochemical impedance spectroscopy (EIS) was used to characteristics before and after graphene modified GCE. The electrochemical impedance spectra measures the impedance of a system over a range of frequencies. In the case of bare graphene, it displays a relatively small electron transfer resistance (Ret) (Figure 2A, curve a) after immobilization of graphene on the electrode's surface. Ret obviously decreases (Figure 2A,

curve b) due to superior electronic transfer ability of graphene to accelerate $[Fe(CN)_6]^{3/4-}$ on the electrode surface [39], confirming successful immobilization.

Figure 2

3.2. Feasibility test: A series of experiments were conducted to investigate the reaction products of DNA in the presence of ExoⅢ and graphene electrodes. Firstly, the gel electrophoresis experiment (Figure. 3A) was performed to characterize DNA hybridization reactions in the presence of ExoⅢ, verifying tetraferrocene-modified short single stranded probe as the product. The double hairpin probe DNA possesses a larger molecular weight, which decreases its movement compared to the target DNA, allowing separation of the band of probe DNA (Lane 1) and target DNA (Lane 2). After hybridization of the target DNA and probe DNA, a new band of greater molecule weight appears, which is ascribed to double stranded DNA formation (Lane 3). The electrophoretic band of the double hairpin DNA and target DNA were incubated in a system with ExoⅢ, releasing a short single strand probe DNA with a smaller molecular weight, which displays a distinct short electrophoresis band moving at a faster rate and three minor electrophoresis bands, which are confirmed by Lane 4. Differential pulse voltammetry was conducted to confirm the obtained results of adsorption of different products. As shown in Figure 2B, when the solution consists of hairpin DNA probe, a relatively small and stable background current is observed (curve a). Upon the addition of 10^{-13} M target DNA, which is expected to open the hairpin probe DNA, a slight increase in DPV signal is found (curve b). Finally, the addition of Exo III triggers a cyclic reaction, promoting significant enhancement of the DPV signal (curve c), demonstrating the ability of graphene to identify the reaction's products. Therefore, the feasibility of the developed DNA biosensor is clearly verified by the above results.

Figure 3

3.3. Comparison of signal amplification of tetraferrocene: In this sensor, we compared the ability of mono- and tetra-ferrocene as signal markers to improve electrochemical signals via labeling of two probes of the same sequence and solution (0.1 pM target DNA and 0.2 U/μl ExoⅢ). Figure 4 displays the oxidation peak of tetraferrocene at a potential of approx. 0.4 V and ferrocene at approx. 0.2 V. This is due to tetraferrocene's greater ferrocene content, allowing

simultaneous oxidation required for higher potential compared with monoferrocene. The highest peak current of DPV indicates that the probe immobilizing tetraferrocene unit is three times greater than monoferrocene, which explains tetraferrocene loss of four electrons on the basis of ferrocene.

Figure 4

3.4. Optimization of experimental conditions: Various conditions were optimized to achieve the maximum detection limit. The concentration of the tetraferrocene probe is important to the performance of the designed biosensor. Low concentrations may result in insufficient target recognition, promoting low detection sensitivity of DNA electrochemical sensor. However, a great quantity of tetraferrocene probe might generate a greater background signal, hence, influencing the performance of the biosensor. 10 nM Concentration of target DNA was employed, and Exo III at 0.2 U/μl. Figure 5A shows that the DPV signal is firstly steady rising with increasing tetraferrocene probe concentration with the maximum signal being obtained after 0.7 μM concentration. Increasing the concentration of the labeled-tetraferrocene probe to 0.8 μM, greatly increased the background signal, therefore 0.7 μM was selected as the optimal dTtFc probe concentration for the biosensor.

Figure 5

The efficiency of signal amplification is mainly derived from Exo III-catalyzed digestion for labeled tetraferrocene probe in DNA double strand. It is well known that Exo III catalytic efficiency relies on the digestion time, reaction temperature and dosage. Figure 5B shows that increasing the digestion time promotes an increase in the electrochemical signal, which reaches maximum after 2 h. As shown in Figure 5C, consider that the DNA hybridization temperature needs to be more than 35 ^{o}C, choose 35 ^{o}C as the starting temperature. Here, we examined the incubation temperature of the Exo III reaction from 35 ^{o}C to 50 ^{o}C. The electrochemical signal increases with increasing incubation temperature, with a maximum temperature of 39 ^{o}C (Figure 5C). After the incubation temperature of the enzyme reaction reached 39 ^{o}C, the DPV signal settled. So, 39 ^{o}C was selected as the optimal reaction temperature. Additionally, optimization of Exo III concentration revealed an increase in electrochemical signal with Exo III, reaching a

plateau after 20 U (Figure 5D) exists in 100µl PBS, which was selected as the optimal reaction concentration for this study.

3.5. Synergistic dynamic response of DNA biosensor: We further assessed the dynamic performance of the biosensor utilizing ExoⅢ and target DNA. In our proposed biosensor, the signal corresponds to the number of target DNA hybridization folding probe and release of tetraferrocene reported under Exo III catalysis. Notably, the tetraferrocene molecule is stable and capable of real-time reflection of surface-confined dynamical molecular configurations. Based on these unique properties, we designed a real-time signal detection system with target DNA and Exo III-assisted. The signal reached saturation at ~150% within 2 h in the presence both of target DNA (10 pM) and Exo Ⅲ (0.2 U/µL). However, the biosensor achieved saturation after 2 h at much lower signal acquisition (~40%) when only target DNA was added. The delay of saturation signal in the coexistence of target DNA and ExoⅢ shows that the synergic reactions between multiple cycles of target, enzymatic digestion and hybrid cycle are occurring.

3.6. Homogenous electrochemical detection of target DNA: To demonstrate the ability of the proposed homogeneous electrochemical DNA biosensor, a series of concentrations of target DNA were measured under the optimized assay conditions. As shown in Figure 6A, a gradual increase in oxidation peak currents value (I_P) of the sensor system is observed with the corresponding increase in target DNA concentration. Target DNA concentrations (C), ranging from 20 fM to 2 nM, are reflected by the peak currents of tetraferrocene. The linear regression equation is I_P = 4.0274 +0.2449 log c, with correlation coefficient of 0.9986. The low detection (target) limit was calculated as 8.2 fM according to the criterion of the signal to noise ratio of 3, which was considerably lower compared with other existing DNA assays [40, 41]. In order to investigate the specificity of the hairpin DNA probe various mismatched target DNA were introduced, control experiments were tested using different DNA sequences (target DNA, single-base-mismatch DNA, three-base-mismatch DNA, and non-complementary DNA) hybridize under the same operating environment described above. Figure 6B illustrates that mismatched completely target DNA produced a negligible DPV signal (signal b), which is similar to the background signal (signal a), one base-mismatched DNA and three base-mismatched DNA produced a very low insignificant DPV signal (signal d, signal c). The complementary sequence (signal e) shows a much higher signal compared to the others. We propose that this sequence specificity toward the

hairpin DNA probe is mainly due to the inherent recognition ability of DNA bases, even its structure is partially opened in the case of hybridization with the target that is not completely complementary, with an obvious steric effect existing for such "hybridizer" to contact the electrode. Therefore, the developed immobilization free electrochemical DNA biosensor can be applied to ultrasensitive detection of target DNA from a sample with high specificity.

Figure 6

3.7 Real sample analysis and reproducibility of biosensors： A preliminary application of the proposed homogeneous electrochemical sensor was performed by detecting the target DNA in the PCR environment to evaluate the analytical reliability and application potential of the proposed sensor. In this work, Cordyceps sinensis gene as a template, PCR was employed to produce a 158 pd single-strand DNA (see Supporting Information (SI) for details). As shown in Figure 7, when our biosensor analyzes target genes from different levels of PCR amplification, the current signal increases as the template concentration increases, and can successfully identify as few as 0.1 pMol/L DNA template in 100 μL unpurified PCR product. This result indicates that our designed sensor has great potential for detecting real samples of DNA.

Figure 7

The inter-batch coefficient of variation (%) was used to study the reproducibility of the biosensor. Inter-batch precision was evaluated by analyzing the same target sample using eight different biosensors prepared independently under the same experimental conditions. The relative standard deviations of 50 fM, 10 pM, and 1000 pM targets in parallel using eight different biosensors were 5.19%, 4.76%, and 4.54%. The experimental results show that the homogeneous electrochemical sensor can be detected and analyzed in real samples, and has good reproducibility.

4. Conclusion

In summary, we developed a multiple-amplified homogeneous electrochemical sensor using graphene as an electrode to accelerate the electron transfer, newly synthesized tetraferrocene as a signal marker and Exo III-assisted for cycling digestion. The application of this electrochemical sensor to rapid and ultra-high sensitive detection target DNA was successfully carried out.

Furthermore, the sensor did not require expensive labeling and tedious probe immobilization processes, DNA hybridization and recognition were performed in homogeneous solution, exhibiting additional advantages of high efficiency and low cost. Therefore, the proposed multiple-amplified homogeneous electrochemical biosensor will become a promising strategy and show great potential in target DNA detection.

Acknowledgements

This work was financially supported by the National Natural Science Foundation of China (81860682, 81872968, 81560625, 81660658), and JiangXi university of traditional Chinese medicine graduate innovation special fund project (JZYC19S02, JZYC19S01).

References

1. F. Patolsky, A. Lichtenstein, I. Willner, J. Am. Chem. Soc, 2001, **123**, 5194-5205.

2. K. Balakin, V. Korshun, I. Mikhalev, G. Maleev, A. Malakhov, I. Prokhorenko, Y. Berlin, Biosens. Bioelectron, 1998, **13**, 771-778.

3. E. O. Blair, D. K. Corrigan, Biosens. Bioelectron, 2019, **134**, 57-67.

4. R. Hu, T. Liu, X. -B. Zhang, S. -Y. Huan, C. Wu, T. Fu, W. Tan, Anal. Chem, 2014, **86**, 5009-5016.

5. C. Wu, S. Cansiz, L. Zhang, I-T. Teng, L. Qiu, J. Li, W. Tan, Am. Chem. Soc, 2015, **137**, 4900-4903.

6. J. Wang, Chem. Eur, 1999, **5**, 1681-1685.

7. E. S. Wong, E. Chow, J. J. Gooding, Langmuir, 2005, **21**, 6957-6965.

8. A. W. Peterson, R. J. Heaton, R. Georgiadis, Am. Chem. Soc, 2000, **122**, 7837-7838.

9. M. I Pividori, A. Merkoci, S. Alegret, Biosens. Bioelectron, 2000, **15**, 291-303.

10. A. K. Geim, K. S. Novoselov, Nat Mater, 2007, **6**, 183-191.

11. G. Brumfiel, Nature, 2009, **458**, 390-391.

12. D. Li, R. B. Kaner, Science, 2008, **320**, 1170-1171.

13. Z. -F. Li, H. Zhang, Q. Liu, L. Sun, L. Stanciu, J. Xie, ACS Applied Materials & Interfaces, 2013, **5**, 2685–2691.

14. Y. Cao, V. Fatemi, S. Fang, K. Watanabe, T. Taniguchi, E. Kaxiras, P. Jarillo-Herrero, Nature, 2018, **556**, 43-50.

15. M. Wang, Q. Yan, F. Xue, J. Zhang, J. Wang, Journal of Physics and Chemistry of Solids,

View Article Online
DOI: 10.1039/D0TB00204F

2018, **119**, 29-35.

16. C. Lee, X. Wei, J. W. Kysar, J. Hone, Science, 2008, **321**, 385-388.

17. C. -H. Lu, H. -H. Yang, C. -L. Zhu, X. Chen, G. -N. Chen, Angew. Chem, 2009, **48**, 4785-4787.

18. X. Xie, K. Zhao, X. Xu, W. Zhao, S. Liu, Z. Zhu, M. Li, Z. Shi, Y. Shao, J Phy Chem C, 2010, **114**, 14243-14250.

19. H. Dong, J. Zhang, H. Ju, H. Lu, S. Wang, S. Jin, K. Hao, H. Du, X. Zhang, Anal. Chem, 2012, **84**, 4587-4593.

20. R. Wang, X. Xu, P. Li, Y. Wang, W. Jiang, Talanta, 2017, **174**, 684-688.

21. S. He, K. -K. Liu, S. Su, J. Yan, X. Mao, D. Wang, Y. He, L. -J. Li, S. Song, C. Fan, Anal. Chem, 2012, **84**, 4622-4627.

22. T. A. Taton, C. A. Mirkin, R. L. Letsinger, Science, 2000, **289**, 1757-1760.

23. C. Schlötterer, Nature Reviews Genetics, 2004, **5**, 63-69.

24. L. Cui, J. Wu, J. Li, H. Ju, Anal. Chem, 2015, **87**, 10635-10641.

25. C. J. Yu, Y. Wan, H. Yowanto, J. Li, C. Tao, M. D. James, C. L. Tan, G. F. Blackburn, T. J. Meade, Am. Chem. Soc, 2001, **123**, 11155-11161.

26. C. Sui, Y. Zhou, M. Wang, H. Yin, P. Wang, S. Ai, S, Sensors and Actuators B: Chemical, 2018, **266**, 514–521.

27. X. Luo, T. M.-H. Lee, I. -M. Hsing, Anal. Chem, 2008, **80**, 7341-7346.

28. Y. Zhang, Y. Wang, H. Wang, J. -H. Jiang, G. -L. Shen, R. -Q. Yu, J. Li, Anal. Chem, 2009, **81**, 1982-1987.

29. C. Fan, K. W. Plaxco, A. J. Heeger, Proceedings of the National Academy of Sciences, 2003, **100**, 9134-9137.

30. E. Xiong, Z. Li, X. Zhang, J. Zhou, X. Yan, Y. Liu, J. Chen, Anal. Chem, 2017, **89**, 8830-8835.

31. Z. Yang, M. A. d'Auriac, S. Goggins, B. Kasprzyk-Hordern, K. V. Thomas, C. G. Frost, P. Estrela, Environmental Science and Technology, 2015, **49**, 5609-5617.

32. A. P. Ferreira, J. L. F. da Silva, M. T. Duarte, M. F. M. da Piedade, M. P. Robalo, S. G. Harjivan, C, Marzano, V. Gandin, M. M. Mardues, 2009, **28**, 5412-5423.

33. H. J. Hwang, J. R. Carey, E. T. Brower, A. J. Gengenbach, J. A. Abramite, Y. Lu, J. Am.

View Article Online
DOI: 10.1039/D0TB00204F

Chem. Soc. 2005, **127**, 15356-15357.

34. W. Z. Yuan, J. Z. Sun, Y. Dong, M. Häussler, F. Yang, H. P. Xu, A. Qin, J. W. Y. Lam, Q. Zheng, B. Z. Tang, Macromolecules, 2006, **39**, 8011-8020.

35. A. E. Finholt, A. C. Bond Jr, H. I. Schlesinger, J. Am. Chem. Soc. 1947, **69**, 1199-1203.

36. R. Appel, Angew. Chem., Int. Ed. Engl, 1975, **14**, 801-811.

37. C. Song, J. Jiao, Q. Lin, H. Liu, Y. He, Dalton Transactions, 2016, **45**, 4563-4569.

38. D. Deng, L. Yu, X. Pan, S. Wang, X. Chen, P. Hu, L. Sun, X. Bao, Chem. Commun, 2011, **47**, 10016-10018.

39. A. Bonanni, M. Pumera, ACS Nano, 2011, **5**, 2356–2361.

40. K. Wang, M. -Q. He, F. -H. Zhai, J. Wang, R. -H. He, Y. -L. Yu, Biosens. Bioelectron, 2018, **105**, 159-165.

41. H. Zhao, D. Ye, X. Mao, F. Li, J. Xu, M. Li, X. Zuo, Biosens. Bioelectron, 2019, **133**, 141-146.

View Article Online
DOI: 10.1039/D0TB00204F

Scheme 1. Schematic illustration of the homogeneous electrochemical DNA sensor for the detection of target.

Scheme 2. The synthetic of 3,5-bis(3, 5-bisferrocenethoxybenzyloxy) benzoic acid (9).

Fig. 1. (A) TEM image and SEM images. **(B)** of graphene sheets.

Fig. 2. (A) Nyquist diagrams obtained at bare GCE (a), graphene modified GCE (b).

Fig. 3. (A) Non-denaturing PAGE confirmation of ExoⅢ assisted target recycling circuit. Lane 1, P1; Lane 2, T1; Lane 3, P1+T1; Lane 4, P1+T1+ExoⅢ. **(B)** Differential pulse voltammetry test of hairpin DNA probe solution: (a) only hairpin DNA probe, (b) hairpin DNA probe and target DNA hybridization, (c) ExoⅢ addition trigger cyclic reaction.

Fig. 4. Comparison of modified probe with different DNA markers.

Fig. 5. The DPV peak current corresponding to different condition settings: **(A)** Concentration of probe; **(B)** Digestion time; **(C)** Temperature; **(D)** ExoⅢ dosage.

Fig. 6. (A) Differential pulse voltammetry recorded with various concentrations of target DNA after hybridization with hairpin probe DNA: 2.0×10^{-14} M, 2.0×10^{-13} M, 2.0×10^{-12} M, 2.0×10^{-11} M, 2.0×10^{-10} M, 2.0×10^{-9} M (b-g) without target DNA (a). (**B**) Comparison of the DPV signal of tetraferrocene when the clamp-probe hybridized with only hybridization buffer containing no DNA sequences (a), 1×10^{-8} M

View Article Online
DOI: 10.1039/D0TB00204F

non-complementary DNA (b), 1×10^{-8} M three base-mismatched DNA (c), 1×10^{-8} M one base-mismatched DNA (d), 1×10^{-10} M target DNA (e).

Fig. 7. Analysis result of PCR products from Cordyceps sinensis DNA by using the biosensor.

Scheme 1

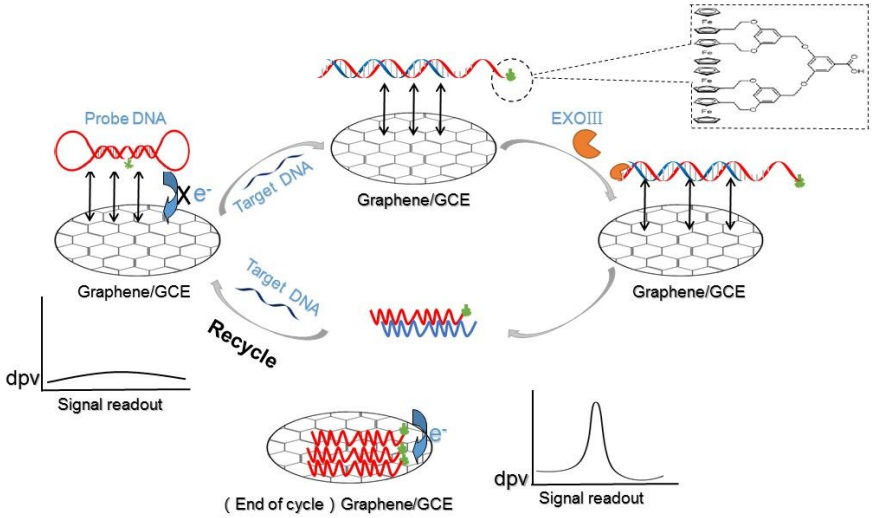

Scheme 2

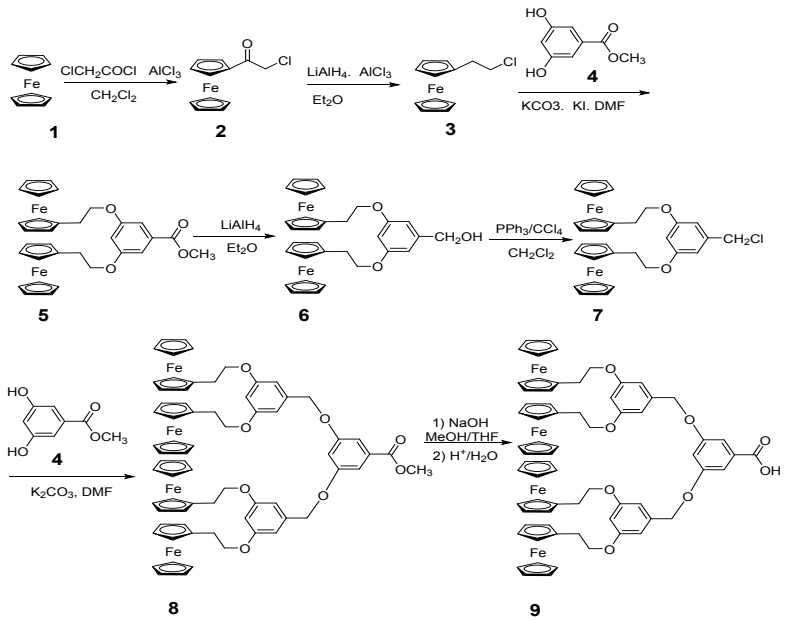

Figure 1

View Article Online
DOI: 10.1039/D0TB00204F

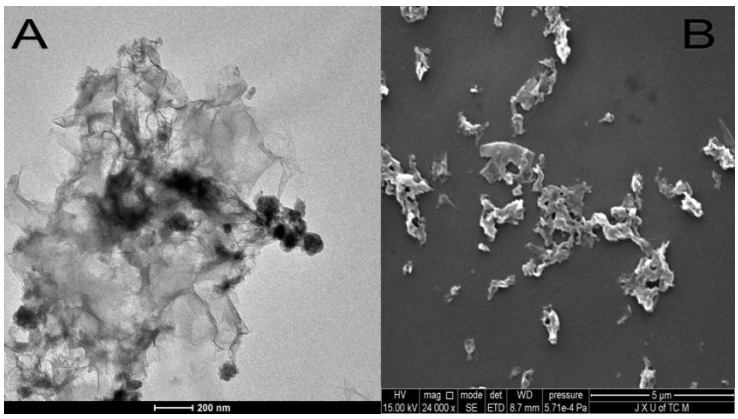

Figure 2

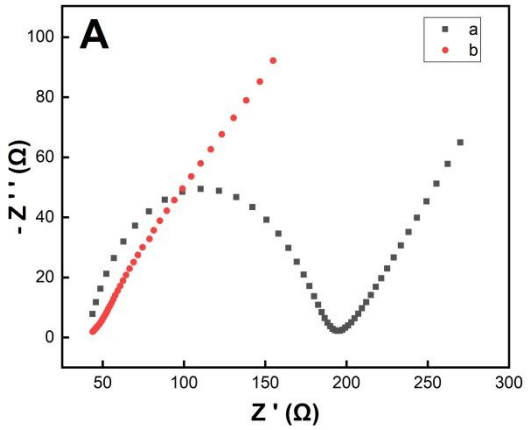

Figure 3

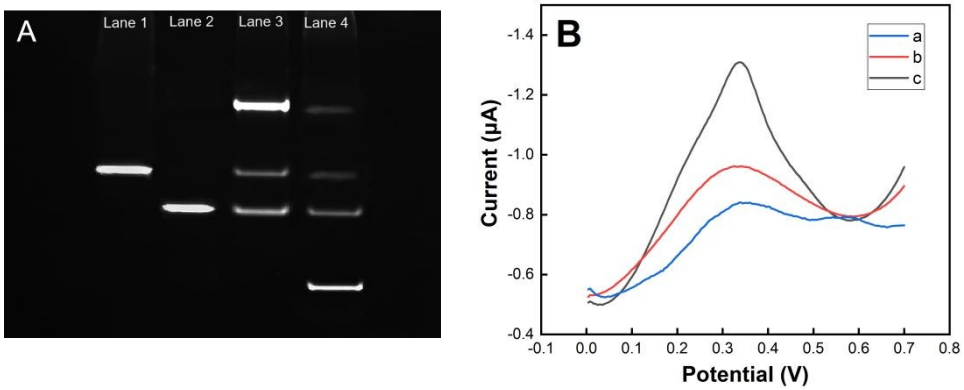

Figure 4

View Article Online
DOI: 10.1039/D0TB00204F

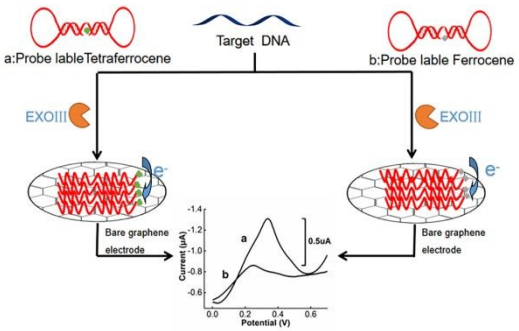

Figure 5

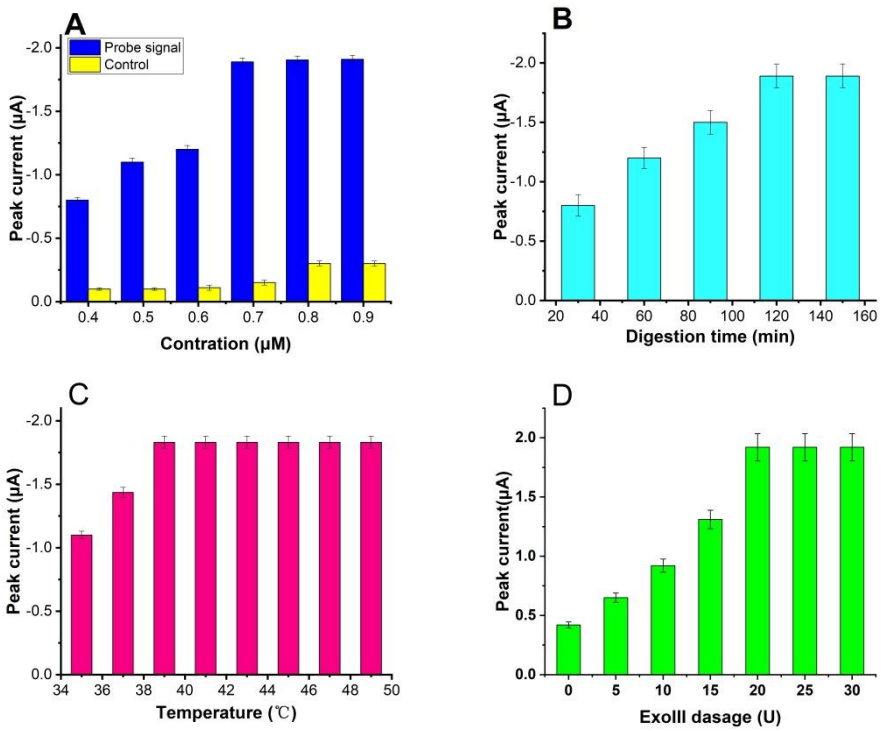

Figure 6

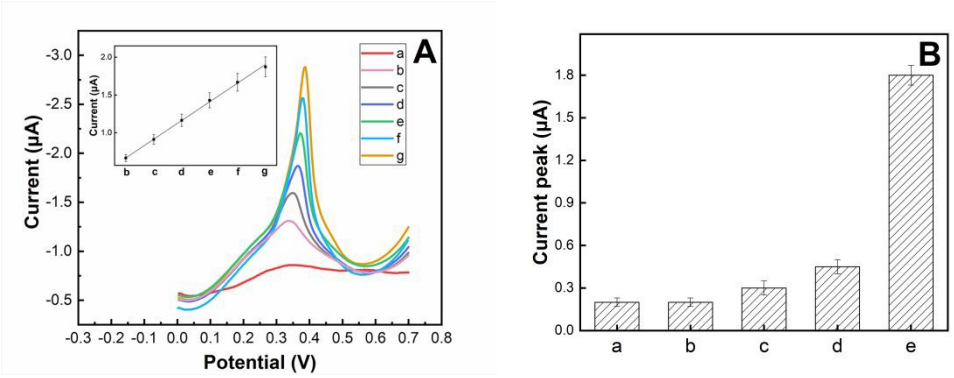

Figure 7

View Article Online
DOI: 10.1039/D0TB00204F